Soil Biology & Biochemistry 94 (2016) 154–168

Contents lists available at ScienceDirect

Soil Biology & Biochemistry

journal homepage: www.elsevier.com/locate/soilbio

Combined use of empirical data and mathematical modelling to better estimate the microbial turnover of isotopically labelled carbon substrates in soil

H.C. Glanville [a, *], P.W. Hill [a], A. Schnepf [c], E. Oburger [b], D.L. Jones [a]

[a] School of Environment, Natural Resources and Geography, Bangor University, Gwynedd LL57 2UW, UK
[b] Department of Forest and Soil Sciences, University of Natural Resources and Life Sciences, Vienna, Konrad-Lorenz Straße 24, A-3430 Tulln, Austria
[c] Forschungszentrum Jülich GmbH, Agrosphere (IBG-3), 52425 Jülich, Germany

ARTICLE INFO

Article history:
Received 26 June 2015
Received in revised form
10 November 2015
Accepted 17 November 2015
Available online 14 December 2015

Keywords:
Amino acids
Decomposition
Dissolved organic carbon (DOC)
Soil organic matter (SOM)
Sugar

ABSTRACT

The flow of carbon (C) through soil is inherently complex due to the many thousands of different chemical transformations occurring simultaneously within the soil microbial community. The accurate modelling of this C flow therefore represents a major challenge. In response to this, isotopic tracers (e.g. ^{13}C, ^{14}C) are commonly used to experimentally parameterise models describing the fate and residence time of individual C compounds within soil. In this study, we critically evaluated the combined use of experimental ^{14}C labelling and mathematical modelling to estimate C turnover times in soil. We applied ^{14}C-labelled alanine and glucose to an agricultural soil and simultaneously measured their loss from soil solution alongside the rate of microbial C immobilization and mineralization. Our results revealed that chloroform fumigation-extraction (CFE) cannot be used to reliably quantify the amount of isotopically labelled $^{13}C/^{14}C$ immobilised by the microbial biomass. This is due to uncertainty in the extraction efficiency values (k_{ec}) within the CFE methodology which are both substrate and incubation time dependent. Further, the traditional mineralization approach (i.e. measuring $^{14/13}CO_2$ evolution) provided a poor estimate of substrate loss from soil solution and mainly reflected rates of internal microbial C metabolism after substrate uptake from the soil. Therefore, while isotope addition provides a simple mechanism for labelling the microbial biomass it provides limited information on the behaviour of the substrate itself. We used our experimental data to construct a new empirical model to describe the simultaneous flow of substrate-C between key C pools in soil. This model provided a superior estimate of microbial substrate use and microbial respiration flux in comparison to traditional first order kinetic modelling approaches. We also identify a range of fundamental problems associated with the modelling of isotopic-C in soil, including issues with variation in C partitioning within the community, model pool connectivity and variation in isotopic pool dilution, which make interpretation of any C isotopic flux data difficult. We conclude that while convenient, the use of isotopic data (^{13}C, ^{14}C, ^{15}N) has many potential pitfalls necessitating a critical evaluation of both past and future studies.

1. Introduction

Soil carbon (C) turnover is a fundamental process in ecosystem functioning. However, understanding the factors regulating soil C dynamics is difficult due to the many hundreds, or even thousands, of processes occurring simultaneously within soil microbial populations (Hanson et al., 2000; Kuzyakov, 2006). A key challenge in ecosystem science is to understand this inherent complexity.

Below-ground respiration represents the primary flux mediating the passage of terrestrial C back to the atmosphere (Van Hees et al., 2005). This flux is dominated by plant (autotrophic) and soil microbe (heterotrophic) respiration. Soil respiration is controlled by the activity of soil microbial communities, which are typically limited by the availability of labile C (Aldén et al., 2001; Glanville et al., 2012). Root exudation (Jones et al., 2009; Nguyen, 2009) and root and mycorrhizal hyphal turnover (Gill and Jackson, 2000; Wallander, 2006) are the main processes by which labile C enters the soil. Within this, low molecular weight (MW) C compounds are of particular importance because, despite representing <10% of

* Corresponding author. Tel.: +44 1248 382456; fax: +44 1248 354997.
E-mail address: h.c.glanville@bangor.ac.uk (H.C. Glanville).

http://dx.doi.org/10.1016/j.soilbio.2015.11.016

total dissolved organic C (DOC), they are postulated to dominate soil CO_2 efflux, due to their rapid rate of production, uptake, assimilation and turnover by the soil microbial community (Jones et al., 2003; Van Hees et al., 2005, 2008). However, it is difficult to gain a detailed mechanistic understanding of how microbial communities mineralize these low MW C substrates as they can undergo a number of fates in soil which are difficult to experimentally separate (e.g. sorption processes and biological transformation).

To accurately model C substrate flow, isotopic tracers (e.g. ^{13}C, ^{14}C) are commonly used to experimentally model the fate and residence time of individual C compounds within soil. In particular, measuring isotopically labelled substrate-derived CO_2 provides an indication as to the speed at which C compounds are specifically biodegraded by the microbial biomass. Measurements of ^{13}C- or ^{14}C-substrate assimilation into the microbial biomass is routinely quantified using the chloroform-fumigation-extraction method of Vance et al. (1987). After extraction of the fumigated sample (e.g. in 0.5 M K_2SO_4), a correction factor (k_{ec}) is applied to the data to account for the fraction of the biomass not soluble in the extractant (e.g. cell walls, insoluble protein; Wu et al., 1990; Joergensen et al., 2011). Correction factors (k_{ec}) applied to microbial biomass data using isotopic tracer studies often vary depending on soil type, soil depth, and rate of substrate addition (Bremer and van Kessel, 1990; Dictor et al., 1998). The k_{ec} value is unlikely to remain constant when using $^{13}C/^{14}C$ pulse-labelled substrates, as the isotopic C becomes progressively transformed within the cells over time (i.e. moves out of the soluble cytosolic pool into insoluble components; Bremer and van Kessel, 1990). In addition, as contrasting C substrates may be partitioned differently within the cell, it is likely that the k_{ec} values also vary significantly between compounds. However, most studies add much higher amounts of labelled substrate than the intrinsic isotopic concentration within the soil solution, therefore stimulating microbial growth and altering partitioning. Here, we directly evaluate the robustness of the k_{ec} approach for tracing isotopically labelled compounds through the soil microbial pool over different chase periods, at native soil solution concentrations not inducing microbial growth.

Combining detailed experimental data with mathematical modelling approaches, can help provide insight into the mechanisms involved in complex processes such as soil C cycling (Roose and Schnepf, 2008). Applying kinetic equations to experimental data makes it possible to parameterise mathematical models, which can then be used to estimate future changes in soil C storage and other key ecosystem services.

First-order reaction kinetics have been used to build a variety of soil organic matter (SOM) decomposition models for over fifty years, mathematically modelling the turnover of multiple C pools within soils and sediments (Salter and Green, 1933; Berner, 1964; Middleburg, 1989; Ostle et al., 2009). First-order reaction kinetics are commonly used for modelling enzyme kinetics and are frequently used within multi-component models describing not only SOM turnover, but also large-scale soil nutrient dynamics (e.g. CENTURY, RothC, ECOSYS; Paul, 2007). Within, this study, we are interested in applying first-order kinetic reaction kinetics to explicitly consider C flows through the soil microbial biomass, focusing specifically on respiration of substrate-derived C from the soluble biomass pool. Commonly, research mainly considers substrate C decomposition by soil microorganisms, rather than specifically including C dynamics within the microbial biomass (Middleburg, 1989; Bosatta and Ågren, 1995; Manzoni et al., 2012). Some other models consider microbial growth and activity when investigating microbial biomass dynamics and apply second order Michaelis-Menton type kinetics. However, these studies often add enough substrate to change the concentration of the intrinsic soil solution pool and stimulate microbial growth (Whitmore, 1996; Nguyen and Guckert, 2001). Here, we directly label the soil solution so as to not induce a microbial growth response beyond that which is naturally occurring, to investigate how C is processed within the microbial biomass.

Following introduction of isotopically labelled low MW compounds into soil, a biphasic pattern of CO_2 evolution is often observed which is suggestive that C can be partitioned into two major compartments/pools (Saggar et al., 1996; Chotte et al., 1998; Boddy et al., 2007). To describe the microbial-driven substrate mineralization kinetics of these two pools, a double first-order exponential decay model is often applied to the experimental data (Boddy et al., 2007). Mineralization experiments using isotopically labelled substrates are conducted over varying time frames; from minutes (Hill et al., 2008; Fujii et al., 2010), days (Coody et al., 1986; Glanville et al., 2012), weeks and years (Simfukwe et al., 2011; Farrar et al., 2012).

However, a two pool model may be too simplistic to describe how some substrates are compartmentalized during their metabolism and a three pool model may describe data more accurately (Hill et al., 2011; Farrar et al., 2012). The first pool of this model is attributed to a rapidly cycled microbial labile C pool (half-lives for this pool reported in minutes/hours; Hill et al., 2008; Farrar et al., 2012; Glanville et al., 2012). The second pool represents microbial structural or stored C (pool half-lives in days/weeks; Boddy et al., 2007; Farrar et al., 2012; Glanville et al., 2012) while the third, slowest turning over pool represents recalcitrant extracellular SOM (pool half-lives in weeks/months; Farrar et al., 2012). In addition, the duration of incubations may influence how pools are attributed to biological function. In particular, for long incubations (months/years), the slowest pool may represent turnover of quasi-stable soil C rather than being representative of microbial C. Further, biological attribution of modelled pools is not only time and substrate specific, but very likely also depends on a range of soil chemical, physical and biological factors (Van Hees et al., 2005).

Even if attribution of biological function to the different pools is achievable, a further major caveat associated with using exponential decay models is the assumed lack of interaction between the discrete pools and the lack of experimental techniques to validate them. To address this issue, we have developed a new empirical model based on our measured pools and applied a set of new, independent equations which allow for interactions between pools.

The first aim of this study was to monitor the temporal dynamics of two contrasting ^{14}C-labelled C substrates through the microbial biomass within an agricultural soil. Secondly, we used this experiment to evaluate whether a single k_{ec} value can be used reliably to assess the amount of substrate-^{14}C contained within the microbial biomass. Thirdly, we used the experimental data to test how the duration of the isotopic tracer experiment influences the choice of modelling approach. Fourthly, we attempted to validate components of the model. Lastly, we used our experimental data to develop a new integrated empirical model (based on measured C pools) which describes the different interactions of C between key pools in soil.

2. Materials and methods

2.1. Field site

Soil was obtained from a hyper-oceanic, freely draining, temperate agricultural grassland located in Abergwyngregyn, Gwynedd, North Wales (53°14′N, 4°1′W). The mean annual rainfall is 1250 mm and the mean annual soil temperature (at 10 cm depth) is 11 °C. The soil is classified as a Dystric Eutrudepts (US Soil Taxonomy). The vegetation at the site consists of perennial ryegrass

(*Lolium perenne* L.) and white clover (*Trifolium repens* L.) and is subject to periodic intensive sheep grazing (>5 ewe ha^{-1}) and receives regular fertilizer addition (120 kg N ha^{-1} y^{-1}). Due to the high root density in the grassland (0.35 ± 0.02 kg m^{-2} in the top 10 cm), all the sampled soil was classified as rhizosphere soil.

2.2. Soil characterisation

Three independent samples of soil (0–10 cm depth) were collected and immediately transferred to the laboratory for analysis (Table 1). The soil passed freely through a 5 mm mesh enabling removal of stones, roots and macro-fauna and ensuring soil homogeneity (Jones and Willet, 2006). Soil water content was measured gravimetrically (24 h at 105 °C). pH and electrical conductivity (EC) were determined in a 1:2.5 (w/v) soil-to-deionised water mixture. Soil solution was extracted within 12 h of soil collection from the field by the centrifugal-drainage method (3200 *g*, 15 min, 20 °C; Giesler and Lundström, 1993). The extracted soil solutions were passed through a 0.22 μm filter and the soil solution stored in polypropylene vials at −20 °C prior to use.

Dissolved organic C (DOC) and total dissolved N (TDN) in soil solution were determined using a TOC-TNV analyzer (Shimadzu Corp., Kyoto, Japan). Ammonium and nitrate were determined colorimetrically following the procedures of Mulvaney (1996) and Miranda et al. (2001) respectively. Dissolved organic nitrogen (DON) was calculated as the difference between TDN and dissolved inorganic N. Total free amino acids (TFAA) were determined by fluorescence using the procedure of Jones et al. (2002). Total free monosaccharides were determined following the 2,4,6-tripyridyl-s-triazine (TPTZ) spectroscopic method of Myklestad et al. (1997). Soil solution P was determined using the molybdate blue method of Murphy and Riley (1962). Total dissolved phenolics were determined following the Folin – Ciocalteu colorimetric method of Velioglu et al. (1998).

2.3. Preparation of isotopically labelled soil solution

Uniformly ^{14}C-labelled D-glucose (Sigma–Aldrich Company Ltd., USA) and L-alanine (Amersham Biosciences, UK) were selected for this study as they represent two common root exudates which are known to be important in soil C cycling (Van Hees et al., 2005). Soil solution was extracted, as described above, and spiked with either ^{14}C-labelled glucose or L-alanine to give a specific activity of ca. 0.9 kBq ml^{-1}. In contrast to many previous studies using high C addition rates, our experiments were designed to replicate substrate concentrations and turnover rates naturally found in the soil. We assume that C flow in the soil was at quasi-steady state and that the concentration of substrate added (<10 nM) did not significantly alter the intrinsic soil solution alanine or glucose concentration and was insufficient to induce microbial growth above that occurring naturally. Then we followed the distribution of the ^{14}C-labelled substrates across five measureable pools over time i.e. the soil solution pool, the exchangeable soil pool, soluble and insoluble microbial pools, and the respired pool. At all times, the sum of the ^{14}C fractions for all pools was equal to 1 (100% of added label).

Table 1
Selected soil properties for the Eutric Cambisol soil used for the mineralization studies. Values represent means ± SEM ($n = 3$).

Soil properties	Topsoil (0–5 cm)
Soil water content (g kg^{-1})	233 ± 3.6
Total C (g C kg^{-1})	25.0 ± 3.30
Total N (g N kg^{-1})	2.70 ± 0.35
C:N ratio	9.24 ± 0.30
Microbial biomass (g C kg^{-1})	2.26 ± 0.35
pH $_{(H2O)}$	5.08 ± 0.01
Electrical conductivity (μS cm^{-1})	113 ± 3.10
Dissolved organic C in soil solution (DOC; mg C l^{-1})	30.7 ± 3.10
Dissolved N in soil solution (mg N l^{-1})	10.8 ± 2.40
Dissolved organic N in soil solution (DON; mg N l^{-1})	3.71 ± 0.28
DOC:DON ratio	7.61 ± 0.12
Free amino acids in soil solution (mg N l^{-1})	0.04 ± 0.01
Free amino acids in soil solution (mg C l^{-1})	0.14 ± 0.02
Free sugars in soil solution (mg C l^{-1})	0.10 ± 0.06
Available NH_4^+ in soil solution (mg N l^{-1})	0.08 ± 0.04
Available NO_3^- in soil solution (mg N l^{-1})	6.67 ± 2.02
Inorganic P in soil solution (mg P l^{-1})	0.24 ± 0.01
Total phenolics in soil solution (mg l^{-1})	0.12 ± 0.04
Soil solution UV absorbance at 254 nm (RAU cm^{-1})[a]	0.43 ± 0.06
Soil solution UV absorbance at 400 nm (RAU cm^{-1})	0.09 ± 0.01

[a] RAU, relative absorbance units.

2.4. Microbial uptake/soil solution pool

The rate of microbial removal of ^{14}C-labelled substrate from soil solution was determined according to Hill et al. (2008). Briefly, 1.7 g of field-moist soil was placed in a 1.5 ml micro-centrifuge tube with a hole pierced through the bottom; this tube was then placed into another intact micro-centrifuge tube. 0.35 ml of ^{14}C-labelled soil solution containing either ^{14}C-glucose or ^{14}C-alanine was added to the soil surface. The soil solution infiltrated immediately through the soil column. Soil solution was collected via centrifugation (4000 *g*, 1 min, 20 °C) after substrate incubation times of 0.5, 1, 2, 4, 8, 12, 24, 48, 168 h and then weekly up to 7 weeks after initial ^{14}C-labelling. Soils were maintained at 20 °C for the duration of the experiment and for all subsequent extractions. The volume of soil solution recovered was recorded and the solution subsequently mixed with Scintisafe 3® scintillation cocktail (Fisher Scientific, UK) and analysed using a Wallac 1404 liquid scintillation counter (Wallac EG&G, UK) to determine its ^{14}C concentration.

2.5. Soil exchange phase/soil sorption pool

To determine the amount of ^{14}C-labelled substrates adsorbed to the soils solid phase ^{14}C-labelled glucose or alanine was added to soil as described above and the soil extracted using 0.5 M K_2SO_4. The amount of ^{14}C in the solution/exchange phase was measured at each time point (as above) by performing a 1:5 (w/v) soil-to-K_2SO_4 (0.5 M) extraction in which the samples were shaken (30 min, 200 rev min^{-1}), centrifuged (18,000 *g*, 5 min) and a 1 ml aliquot of the supernatant retained for ^{14}C analysis as described above.

2.6. Soluble microbial biomass extraction

To determine the amount of ^{14}C retained within the soluble fraction of the microbial biomass, ^{14}C-labelled glucose or alanine was added to the soil as described above. At the sampling times shown in Section 2.4, the soil was fumigated with chloroform (Vance et al., 1987) for 24 h in the dark at 20 °C. After fumigation, the samples were extracted with 0.5 M K_2SO_4 (1:5 w/v) as described above for the non-fumigated samples.

2.7. Microbial biomass not extracted by K_2SO_4/methanol extractable microbial biomass

To investigate the organic solvent extractable fraction of ^{14}C-labelled substrate still retained in the microbial biomass, soil remaining after $CHCl_3$-fumigation was re-suspended in methanol (MeOH). Briefly, the excess K_2SO_4 was removed from the soil and replaced with 100% methanol (1:5 w/v) and the soils shaken (30 min, 200 rev min^{-1}), centrifuged (18,000 *g*, 5 min) and 1 ml of

the supernatant recovered for ^{14}C determination as described above.

2.8. Substrate-C mineralization

To measure the rate of substrate mineralization, 1.7 g of soil was placed in a 1.5 ml micro-centrifuge tube placed inside a sealable 50 ml polypropylene cylinder, and 0.35 ml of soil solution containing ^{14}C-labelled glucose or alanine added to the soil surface. After addition, a NaOH trap (1 ml, 1 M) was added and the cylinders sealed. NaOH traps were changed and their ^{14}C content determined as described in Section 2.4. To determine the amount of ^{14}C still remaining in the soil after 7 weeks, soil which had not been subjected to the extraction or fumigation steps described above, was combusted in an OX400 biological oxidiser (R.J. Harvey Instrument Corp., USA) and $^{14}CO_2$ measured by scintillation counting after capture in Oxosol scintillant (National Diagnostics, Atlanta, GA, USA).

2.9. Traditional modelling approach for describing ^{14}C dynamics in soil

Traditionally, models describing C dynamics use first-order kinetics to obtain a series of decay constants that best represent substrate decomposition by microbial communities (Berner, 1964; Middleburg, 1989; Harakuk et al., 2015). These decay constants represent only a composite of the multitude of processes that occur simultaneously within the microbial "black box", and as such often over−simplify complex microbial processes (Allison and Martiny, 2008). To describe ^{14}C soil dynamics, often exponential decay models are used to estimate microbially-driven substrate mineralization rates (Chotte et al., 1998; Van Hees et al., 2005; Boddy et al., 2007).

Nguyen and Guckert (2001) and Farrar et al. (2012) suggested that glucose mineralization follows a triphasic pattern which can be described by a triple exponential decay model:

$$f(t) = a_1 \times \exp^{-k_1 t} + a_2 \times \exp^{-k_2 t} + a_3 \times \exp^{-k_3 t} \quad \text{(Eqn. 1)}$$

where $f(t)$ is the amount of ^{14}C remaining in the soil at time t, a_1, a_2 and a_3 describe the initial size of each respective pool, and k_1, k_2 and k_3 correspond to the exponential decay constants for each respective pool. The first phase (k_1) is thought to correspond to $^{14}CO_2$ efflux as substrates are immediately used for catabolic processes (i.e. respiration) (Boddy et al., 2007). The second pool (a_2) relates to a slower mineralization phase (k_2) attributable to C temporarily immobilized within the biomass (i.e. storage-C). The third pool (a_3) probably relates to the very slow breakdown (k_3) of microbial structural-C compounds and C chemically and/or physically protected in soil (Farrar et al., 2012).

Alternatively, a first-order double exponential decay model (biphasic mineralization pattern) may be used to describe substrate mineralization:

$$f(t) = a_4 \times \exp^{-k_4 t} + a_5 \times \exp^{-k_5 t} \quad \text{(Eqn. 2)}$$

Where, a_4 and a_5 describe the size of each respective pool, and k_4 and k_5 correspond to the exponential decay constants for each mineralization phase. Here, the first pool (a_4) is thought to correspond to a C pool which is rapidly used (k_4) for catabolic processes (i.e. comparable to pool a_1 in the triphasic model). The second, more recalcitrant pool (a_5) probably constitutes the remaining C immobilized within the microbial biomass (i.e. used for cell growth and maintenance) or necromass which turns over much more slowly (k_5).

The half-life ($t_{½}$) for the first mineralizable pool from both models (a_1 and a_4) can be calculated as follows:

$$t_{½} = \ln(2)/k \quad \text{(Eqn. 3)}$$

Calculating the half-life for the slower second and third pools is probably unreliable as the double and triple models assume the different pools are unconnected (see Discussion).

Eqns. (1) and (2) cannot be solved explicitly for t and so the Newton−Raphson algorithm was applied to both the double and triple exponential decay equations to calculate the time when the overall ^{14}C remaining in the soil is half the initial amount; from here on this is referred to as the substrate halving-time.

To describe the removal of ^{14}C-substrate from soil solution, a first-order model with asymptote was fitted to the data;

$$f(t) = y_0 + \left(a_6 \times \exp^{-k_6 t}\right) \quad \text{(Eqn. 4)}$$

where y_0 represents the maximum depletion of ^{14}C from the soil solution pool, a_6 describes initial size of the bioavailable soil solution ^{14}C pool and k_6 is the exponential rate constant describing the turnover rate of this second pool. A two pool model was also fitted to the experimental data describing the dynamics of the 0.5 M K_2SO_4 extractable pool (^{14}C-substrate adsorbed to the soil phase). Here y_0 represents the maximum depletion of ^{14}C from the soil sorption pool, with a_6 replaced by a_7 to describe the size of the initial pool and k_6 replaced by k_7 for the exponential rate constant for this pool. The half-lives were calculated according to Eqn. (5), with a_7 and k_7 replacing a_6 and k_6 for the K_2SO_4 extractable pool. It is worth noting that this equation calculates the overall half-life, however, when $y_0 > a_6$ or a_7 then the substrate will never be reduced to half and therefore Eqn. (5) would have no solution.

$$t_{½} = \ln(2 \times a_6/(a_6 - y_0))/k_6 \quad \text{(Eqn. 5)}$$

To describe changes in the K_2SO_4-soluble ^{14}C-labelled microbial biomass pool ($CHCl_3$-fumigation) and the MeOH extractable (K_2SO_4-insoluble) microbial biomass pool, a first-order double exponential decay equation (Eqn. (2); two pool model) was fitted to the experimental data. Here, a_8 and a_{10} likely represent the more soluble components of the microbial biomass ($CHCl_3$-fumigation and K_2SO_4-insoluble extractions respectively). Pools a_9 and a_{11} may describe the more insoluble microbial components ($CHCl_3$-fumigation and K_2SO_4-insoluble extractions respectively) which require further breakdown from extra-cellular enzymes to become remobilised and before passing into the more soluble pool prior to microbial utilization. Rate constants for each pool are defined by k_8, k_9, k_{10} and k_{11} respectively.

$CHCl_3$ fumigation efficiency values (k_{ec}) were calculated as follows:

$$k_{ec} = \frac{F}{(100 - R - Ss - S)} \quad \text{(Eqn. 6)}$$

where k_{ec} is defined as the correction factor value to account for the amount of microbial biomass ^{14}C not extractable with K_2SO_4. F is the percent of ^{14}C-labelled substrate extracted from the soluble microbial biomass pool by $CHCl_3$ fumigation-extraction, R is the percent of ^{14}C-labelled substrate respired, S_s is the percent of ^{14}C-labelled substrate remaining in soil solution. Finally, S is the amount of ^{14}C-labelled substrate sorbed to soil particles (after accounting for that recovered in soil solution). Here, we assume that there is minimal transfer of microbial-^{14}C to stable soil organic matter, particularly over the first few days of the experiment.

2.10. New model to describe processing of labelled low MW C substrates within the microbial biomass

A new empirical model is proposed here which incorporates interaction pathways between different pools identified within the model (Fig. 1), which is something both the first-order double and triple exponential decay models fail to account for. For both alanine and glucose, microbial substrate decomposition was modelled over time using a new and independent set of equations, and outputs are expressed as a percentage of the total specific activity added to the soil.

We define five C pools based on the measured pools of ^{14}C, i.e. C_l, the ^{14}C-labelled substrate in soil solution, C_s, the ^{14}C-substrate adsorbed to the soil solid phase, $C_{m,sol}$, soluble ^{14}C contained in the microbial biomass, $C_{m,ins}$, insoluble ^{14}C contained in the microbial biomass, and C_{resp}, respired $^{14}CO_2$.

We assume that there is flow of ^{14}C between those pools as shown in Fig. 1. Substrate added to the soil solution can either be adsorbed to the soils solid phase or it can be taken up into the soluble microbial biomass pool. There are fluxes in both directions to and from the soluble and insoluble microbial biomass pools. We assume that respiration can only occur from the soluble microbial biomass pool. The composition of the microbial community as well as the substrate quality can change over time; therefore, the respiration rate constant can also vary over time (Bosatta and Ågren, 1995; Manzoni et al., 2012). As such, we assume that the respiration rate constant is inversely proportional to time, with initially rapid respiration that slows down with time.

Conservation of mass leads to the following system of equations (Eqns. (7)–(17) are completely independent from Eqns. (1)–(6)):

$$\frac{dC_l}{dt} = -k_{upt}C_l - k_aC_l + k_dC_s \quad \text{(Eqn. 7)}$$

$$\frac{dC_s}{dt} = k_aC_l - k_dC_s \quad \text{(Eqn. 8)}$$

$$\frac{dC_{m,sol}}{dt} = k_{upt}C_l - k_{res}(t)C_{m,sol} - k_{ins,f}C_{m,sol} + k_{ins,b}C_{m,ins} \quad \text{(Eqn. 9)}$$

$$\frac{dC_{m,ins}}{dt} = k_{ins,f}C_{m,sol} - k_{ins,b}C_{m,ins} \quad \text{(Eqn. 10)}$$

$$\frac{dC_{resp}}{dt} = k_{res}(t)C_{m,sol} \quad \text{(Eqn. 11)}$$

where k_{upt} (day^{-1}) is the uptake rate constant from soil solution into soluble biomass pool, $k_{ins,f}$ (day^{-1}) is the forward reaction rate constant describing the flow of C from the soluble to insoluble biomass pool. $k_{ins,b}$ (day^{-1}) is the backward reaction rate constant describing C flow from the insoluble to soluble biomass pool. $k_{res}(t) = k_{res\_c}/(t + b)$ is the time dependent respiration rate constant where the parameters k_{res_c} (dimensionless), t is time (days) and b (days) determine the shape of this time dependence, k_a (day^{-1}) is the adsorption rate constant, and k_d (day^{-1}) is the desorption rate constant.

2.11. Parameter estimation

Parameters and 95% confidentiality bounds were determined using the Matlab function lsqcurvefit in three steps:

1. In an independent experiment on sterile soil (data not presented), we measured the kinetics of substrate sorption, based on methods described by Barber (1984), in order to determine the sorption rate constants k_a and k_d. As there are no microbes present in sterile soil, the two pools of interest are now only the liquid and sorbed phase. Assuming linear sorption, the equations are given by:

$$\frac{dC_l}{dt} = -k_aC_l + k_dC_s \quad \text{(Eqn. 12)}$$

$$\frac{dC_s}{dt} = k_aC_l - k_dC_s \quad \text{(Eqn. 13)}$$

This is a system of linear differential equations with constant coefficients and can be solved analytically. For initial conditions (C_l, C_s) = (100,0), the solutions are:

$$C_l = 100 - \frac{100k_a}{k_a + k_d}\left(1 - e^{-(k_a+k_d)t}\right) \quad \text{(Eqn. 14)}$$

$$C_s = \frac{100k_a}{k_a + k_d}\left(1 - e^{-(k_a+k_d)t}\right) \quad \text{(Eqn. 15)}$$

Eqn. (14) was then fitted to the measured data in order to obtain the sorption rate constants k_a and k_d.

2. Moving back to non-sterile soil and assuming that the sorption rate constants will not change whether the soil is sterile or not, the uptake rate constant can be determined by fitting the following equations solely to the data from the C_l and C_s pools in the main experiment.

$$\frac{dC_l}{dt} = -k_{upt}C_l - k_aC_l + k_dC_s \quad \text{(Eqn. 16)}$$

$$\frac{dC_s}{dt} = k_aC_l - k_dC_s \quad \text{(Eqn. 17)}$$

3. The remaining parameters k_{upt}, $k_{ins,f}$, $k_{ins,b}$, k_{res_c}, and b were determined by fitting the full model to the data of all pools of the main experiment.

2.12. Statistical and data analysis

All experiments were carried out in triplicate and data visually inspected for normality using quantile–quantile plots (Crawley, 2007). All statistical procedures were carried out using the statistical package 'R' v 2.12.1 (2010), with $P = 0.05$ used as the upper limit for statistical significance. Non-normally distributed data were log-transformed prior to analysis. A two-sample student's t-test was used to compare the different model parameters. Exponential decay curves were fitted to the experimental data using a least squares iterative model in SigmaPlot v12.3 (Systat Software Inc., USA). Dependency values for each model parameter were used to indicate whether the parameter values were strongly dependent on one another. To critically evaluate which decay model best described the experimental data, the following criteria were employed: An r^2 value of 0.90 was deemed acceptable for assessing the fit of the model to the experimental data. To check for model over-fitting, a dependency value cut-off of 0.98 was selected (Farrar et al., 2012). Further, a least-squares estimation (LSE) was calculated to evaluate the accuracy of the estimation of parameter values (Wolfe and Chinkes, 2005).

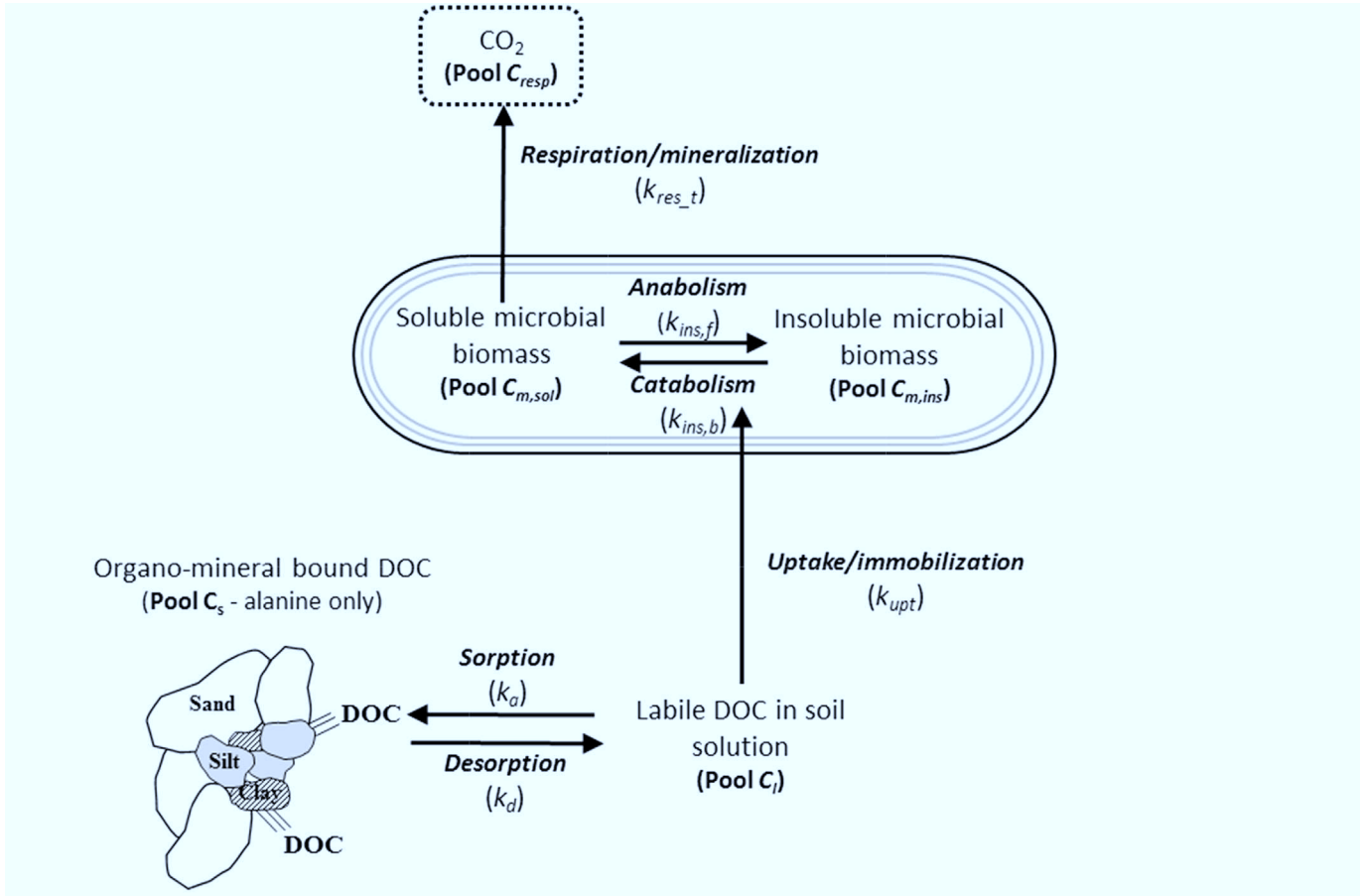

Carbon pools used within the model:
C_l: Labile C present within soil solution (i.e. DOC).
C_s: C sorbed to the solid phase (this pool only applies for alanine as there are no known mechanisms for glucose sorption to occur (Fischer et al., 2010; Kuzyakov and Jones, 2006).
$C_{m,\,sol}$: C within the soluble component of the microbial biomass.
$C_{m,\,ins}$: C within the insoluble component of the microbial biomass.
C_{resp}: CO_2 respired from the microbial biomass.

Rate constant derived from the model:
k_{upt} (day^{-1}): uptake rate constant from soil solution into soluble biomass pool
$k_{ins,f}$ (day^{-1}): forward reaction rate constant describing flow from soluble to insoluble biomass pool
$k_{ins,b}$ (day^{-1}): backward reaction rate constant describing flow from insoluble to soluble biomass pool
k_{res_c} (-): respiration rate constant from soluble biomass to respired CO_2 pool
b (days): parameters for time dependence of respiration rate constant:

$$k_{res\_t} = k_{res\_c} / (t + b)$$

Alanine has in addition the parameters for sorption in soil:
k_a (day^{-1}): adsorption rate constant
k_d (day^{-1}): desorption rate constant

Fig. 1. Conceptual model of C pools defined within a new model to estimate contributions to soil microbial respiration. The C pools are provisionally attributed after performing extractions on soils spiked with ^{14}C-labelled glucose and alanine. The rate constants (k values) are those outputs associated with the new model and have been assigned to exchanges (arrows) which we hypothesize best reflect their associated pool. For the catabolic exchange ($k_{ins,b}$), it is possible this may also include transfer via the labile DOC pool, but this exchange was not directly measured and so is not included within this figure. For a full description of model parameters, see Materials and Methods.

To evaluate how increasing the number of data points in the mineralization experiment influenced the choice of kinetic model, we compared model fits using a minimum of 6, up to a maximum of 15 individual data points. Six was chosen as the minimum number because this represented the number of parameters in the triphasic model. Further, we investigated whether the pools/compartments assigned after fitting a kinetic model to the $^{14}CO_2$ evolution data correspond to the different operationally defined measurements (chemical extracts) of the known mineralizable pools. This could provide biological justification of the chosen mathematical model.

3. Results

3.1. Microbial uptake/soil solution pool

The depletion of ^{14}C-substrate from the soil solution was extremely rapid and the first order single exponential model with asymptote fitted well to the data (Fig. 2a; $r^2 > 0.99$ for both substrates). After the initial sampling, levels of ^{14}C recovered in soil solution were low throughout the experiment for both substrates (Fig. 2a, Fig. S1). The half-life for both alanine and glucose in soil

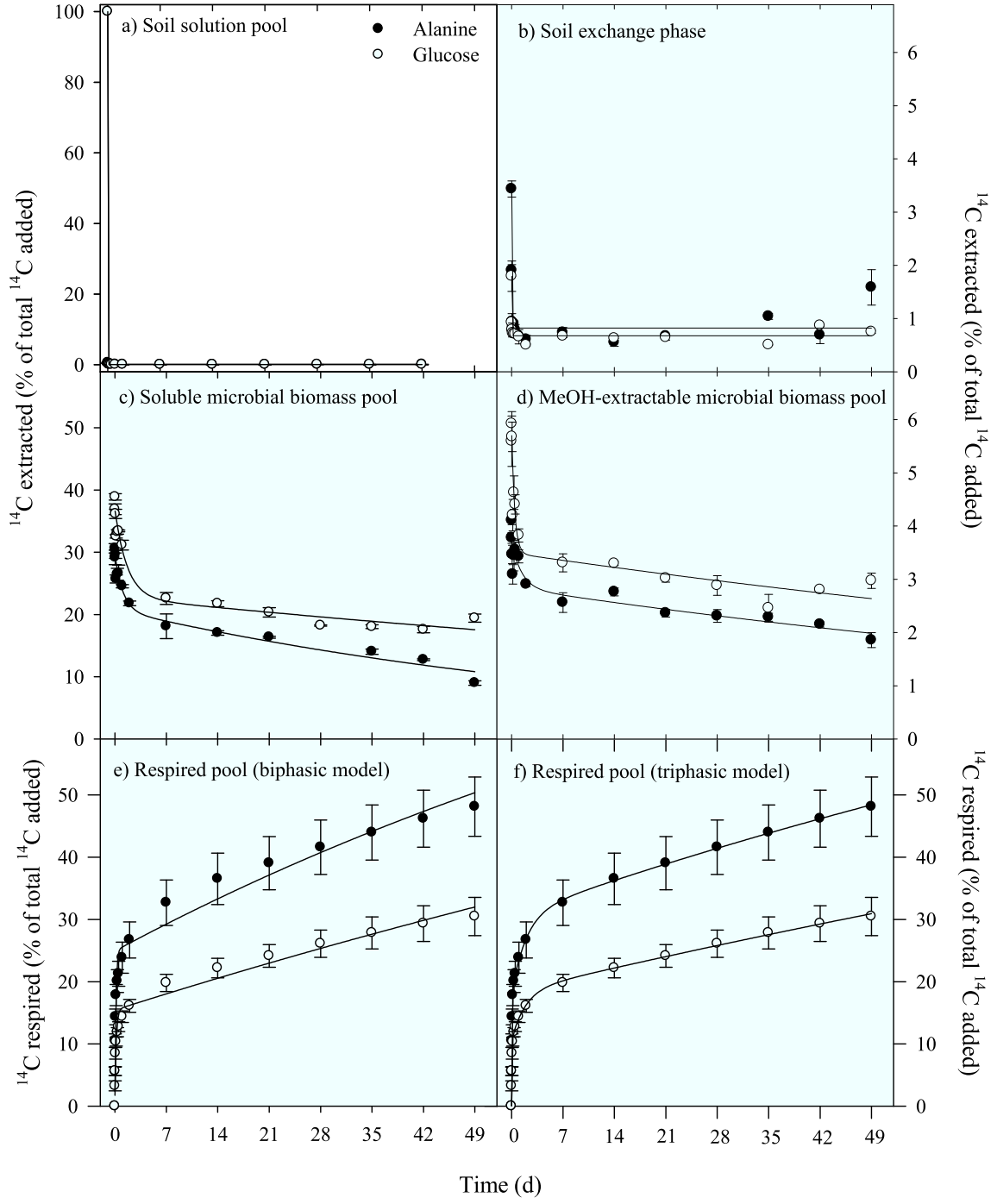

Fig. 2. Amount of ^{14}C recovered from different chemical extractions (panels a to d) and cumulative microbial respiration (panels e and f) after addition of ^{14}C-labelled alanine or glucose to an agricultural grassland soil. Values represent means ± SEM ($n = 3$). Lines represent model fits. Panel e shows model fits for the double first order kinetic equation and f is for the triple first order kinetic equation. Note different y-axis scales for each panel.

solution was estimated to be very short at 4.3 ± 0.3 min (Tables 2 and 3). The amount of ^{14}C recovered in the soil solution pool after 49 d was very low (0.09 ± 0.04 and 0.02 ± 0.008% of the total ^{14}C activity added for alanine and glucose respectively).

3.2. Soil exchange phase/soil sorption pool

After accounting for the ^{14}C recovered in soil solution, the amount of ^{14}C recovered in the 0.5 M K_2SO_4 soil extracts was also very low (Fig. 2b, Fig. S1). This loss of ^{14}C from soil exchange sites was well described by a single exponential decay with asymptote model ($r^2 > 0.89$ for both substrates). The half-lives for substrates within this K_2SO_4 extractable pool were very short being 0.5 ± 0.2 h and 1.2 ± 0.5 h for alanine and glucose respectively (Tables 2 and 3).

3.3. Soluble microbial biomass extraction

The $CHCl_3$ fumigation-extractable microbial biomass pool contained a larger amount of ^{14}C in the glucose treatment in comparison to alanine throughout the experiment ($P < 0.05$ for all time points, except 48 h where $P > 0.05$; Fig. S1). The amount of ^{14}C recovered by $CHCl_3$ fumigation-extraction was well described by a first order double exponential decay model (Fig. 2c; $r^2 = 0.97$ for both substrates). The first modelled pool (a_8) for glucose had almost a third more ^{14}C allocated to it compared to alanine ($P < 0.01$; Tables 2 and 3). However, the rate constant (k_8) and half-life describing loss of ^{14}C from this pool showed no difference between substrates ($P > 0.05$).

3.4. $CHCl_3$ fumigation-extraction efficiency (k_{ec}) values

When including all measured ^{14}C pools, approximately 50% of the added ^{14}C remained unrecovered for both substrates (Fig. 3ab). Over 49 d, the amount of unrecovered ^{14}C stayed relatively constant in the glucose treatment (ca. 50%) but showed a progressive decline in the alanine treatment (Fig. 3ab). If the widely accepted extraction efficiency factor was used ($k_{ec} = 0.45$; Vance et al., 1987), the calculated total ^{14}C in the biomass after 24 h, increased from approximately 50% to 80% and 84% for alanine and glucose respectively. From our data, however, we empirically calculated the k_{ec} values to be 0.35 and 0.36 ± 0.01 for alanine and glucose respectively at 24 h (Fig. 3cd). These k_{ec} values decreased over time and after 49 d, the values had fallen to 0.21 and 0.28 ± 0.01 for alanine and glucose respectively (Fig. 3cd).

3.5. Microbial biomass not soluble in K_2SO_4/Methanol extractable microbial biomass

More ^{14}C was recovered by MeOH extraction in the glucose treatment in comparison to alanine over 49 d ($P < 0.05$; Fig. 2d). The recovery of ^{14}C in the MeOH extraction was well described by a first order double exponential decay model (Fig. 2d; $r^2 > 0.90$ for both substrates). The MeOH-extractable microbial biomass fraction did not differ statistically between substrates, constituting 2.88 ± 0.28% and 4.82 ± 0.75% of the non-mineralized pool, obtained after biological oxidation for alanine and glucose respectively after 49 d.

3.6. ^{14}C-Substrate mineralization

More ^{14}C-alanine was recovered as $^{14}CO_2$ compared to glucose ($P < 0.05$; Fig. 2ef). The mineralization data for both alanine and glucose fitted well to both double and triple exponential decay models with dependency levels for all parameters well below the critical 0.98 cut-off threshold (Fig. 2ef, Table 4). Overall, however, the double exponential decay model gave a poorer fit to the experimental data over the entire dataset. It is worth noting that, irrespective of the number of data points used in the analysis, both substrates showed strong model fits to the experimental data for both double and triple exponential decay models ($r^2 > 0.995$). Dependency values for all model parameters, again for both double and triple exponential decay models, were highest at the beginning of the experiment and declined over time (with inclusion of greater numbers of data points). Overall, however, the dependency values were significantly higher for the triple decay model than for those

Table 2
Model parameters describing the size and turnover of the extractable ^{14}C pool for alanine over time. The models are described by single, double or triple exponential decay equations (see Materials and Methods for further details). Only the single decay equations were fitted with an asymptote (asym.). Values represent means ± SEM ($n = 3$), n.a. indicates not applicable, letters and values in brackets denote individual model parameters. Pools were assigned to each extractable ^{14}C pool, with the NaOH traps representing a respired pool (triple exponential decay model only), the centrifuged soil solution represents the labile soil solution pool, K_2SO_4 extracts are ascribed to the substrate held on the exchangeable phase (sorption pool), $CHCl_3$-fumigation and MeOH extracts represent the soluble and more insoluble pool of the microbial biomass pool respectively.

Extraction method and associated model – Alanine					
Model parameters (% values refer to % of total ^{14}C added)	NaOH trap (Triple exponential decay model)	Centrifuged soil solution (Single exponential decay model with asym.)	K_2SO_4 extract (Single exponential decay model with asym.)	$CHCl_3$ fumigation (Not K_{ec} corrected) (Double exponential decay model)	MeOH extract (Double exponential decay model)
Asymptote pool – (%)	n.a.	0.14 ± 0.01 (y_0)	0.67 ± 0.01 (y_0)	n.a.	n.a.
Pool 1 – (%)	18.0 ± 1.47 (a_1)	99.9 ± 0.01 (a_6)	6.08 ± 0.37 (a_7)	8.88 ± 0.46 (a_8)	0.89 ± 0.16 (a_{10})
Pool 1 rate constant – (h^{-1})	0.77 ± 0.05 (k_1)	11.3 ± 0.89 (k_6)	1.59 ± 0.01 (k_7)	0.04 ± 0.01 (k_8)	0.19 ± 0.15 (k_{10})
Pool 1 half-life (d)	0.04 ± 2.0 × 10^{-3}	3.0 × 10^{-3} ± 2.0 × 10^{-4}	0.02 ± 1.0 × 10^{-4}	0.79 ± 0.20	0.58 ± 0.27
Pool 2 – (%)	12.6 ± 2.09 (a_2)			20.7 ± 1.41 (a_9)	3.01 ± 0.02 (a_{11})
Pool 2 rate constant – (h^{-1})	2.1 × 10^{-2} ± 2.1 × 10^{-4} (k_2)			5.7 × 10^{-4} ± 8.8 × 10^{-5} (k_9)	4.0 × 10^{-4} ± 5.8 × 10^{-5} (k_{11})
Pool 2 half-life – (d)	1.35 ± 0.01			53.9 ± 9.38	75.4 ± 11.2
Pool 3 – (%)	69.4 ± 3.59 (a_3)				
Pool 3 rate constant – (h^{-1})	2.3 × 10^{-4} ± 3.3 × 10^{-5} (k_3)				
Pool 3 half-life – (d)	128.4 ± 16.0				
Total substrate halving-time (d) (Newton–Raphson algorithm)	62.7 ± 16.1	0.003 ± 2.0 × 10^{-4}	0.02 ± 4.0 × 10^{-4}	24.9 ± 1.36	47.8 ± 7.46
Assigned pool	Respired pool	Labile soil solution pool	Soil sorption pool	Soluble microbial biomass pool	MeOH extractable microbial biomass pool

Table 3
Model parameters describing the size and turnover of the extractable ^{14}C pool for glucose over time. The models are described by single, double or triple exponential decay equations (see Materials and Methods for further details). Only the single decay equations were fitted with an asymptote (asym.). Values represent means ± SEM ($n = 3$), letters and values in brackets denote individual model parameters. Pools were assigned to each extractable ^{14}C pool, with the NaOH traps representing a respired pool, the centrifuged soil solution represents the labile soil solution pool, K_2SO_4 extracts are ascribed to substrate held on the exchangeable phase (sorption pool), $CHCl_3$-fumigation and MeOH extracts represent the soluble and more insoluble pool of the microbial biomass pool respectively.

Extraction method and associated model – Glucose					
Model parameters (% values refer to % of total ^{14}C added)	NaOH trap	Centrifuged soil solution	K_2SO_4 extract	$CHCl_3$ fumigation (not K_{ec} corrected)	MeOH extract
	(Triple exponential decay model)	(Single exponential decay model with asym.)	(Single exponential decay model with asym.)	(Double exponential decay model)	(Double exponential decay model)
Asymptote pool – (%)	n.a.	0.06 ± 0.01 (y_0)	0.61 ± 0.001 (y_0)	n.a.	n.a.
Pool 1 – (%)	10.7 ± 0.61 (a_1)	99.9 ± 0.01 (a_6)	0.66 ± 0.30 (a_7)	14.0 ± 0.62 (a_8)	2.37 ± 0.27 (a_{10})
Pool 1 rate constant – (h^{-1})	0.73 ± 0.14 (k_1)	11.1 ± 0.40 (k_6)	0.46 ± 0.33 (k_7)	$0.03 \pm 3.0 \times 10^{-3}$ (k_8)	0.10 ± 0.03 (k_{10})
Pool 1 half-life (d)	0.04 ± 0.01	0.003 ± 9.5 × 10^{-5}	0.05 ± 0.01	1.15 ± 0.11	0.34 ± 0.09
Pool 2 – (%)	7.79 ± 0.46 (a_2)			22.8 ± 0.99 (a_9)	3.45 ± 0.11 (a_{11})
Pool 2 rate constant – (h^{-1})	2.2×10^{-2} ± 4.6×10^{-4} (k_2)			2.3×10^{-4} ± 6.7×10^{-5} (k_9)	1.7×10^{-4} ± 3.3×10^{-5} (k_{11})
Pool 2 half-life – (d)	1.47 ± 0.35			160.5 ± 64.2	192.5 ± 48.1
Pool 3 – (%)	81.5 ± 0.91 (a_3)				
Pool 3 rate constant – (h^{-1})	1.6×10^{-4} ± 4.0×10^{-5} (k_3)				
Pool 3 half-life – (d)	217.2 ± 72.8				
Total substrate halving-time (d) (Newton–Raphson algorithm)	154.4 ± 54.1	0.003 ± 9.5 × 10^{-5}	0.05 ± 0.02	44.3 ± 10.3	36.3 ± 6.04
Assigned pool	Respired pool	Labile soil solution pool	Soil sorption pool	Soluble microbial biomass pool	MeOH extractable microbial biomass pool

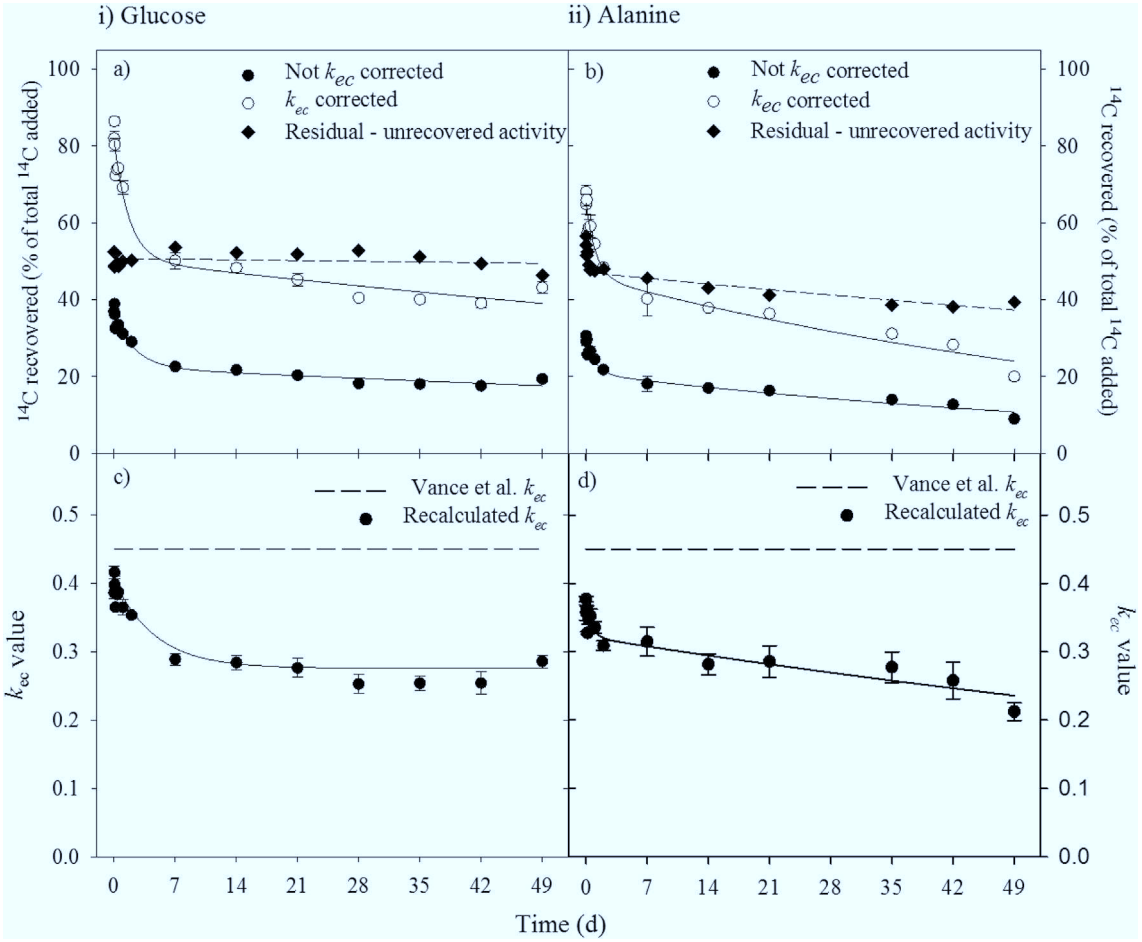

Fig. 3. Time-dependent microbial immobilization of ^{14}C derived from both ^{14}C-labelled glucose and alanine. Panels a and b show the differences in amount of recoverable ^{14}C with and without the inclusion of the constant k_{ec} factor from Vance et al. (1987), alongside the residual activity remaining after the different extractions. Panels c and d show how the constant correction factor of 0.45 (of Vance et al., 1987) compares with our experimentally derived k_{ec} values (calculated by combining results from a series of different extractions of known mineralizable pools).

Table 4
Parameter estimates and dependency values from two different exponential decay models describing the mineralization of alanine and glucose in a Eutric Cambisol soil. Values represent means ± SEM for each substrate ($n = 3$).

	Model parameters	Double exponential decay model	Dependency values	Triple exponential decay model	Dependency values
Alanine	a_1 (%)	22.6 ± 2.17	0.50 ± 0.013	18.0 ± 1.47	0.68 ± 0.017
	k_1 (h^{-1})	0.31 ± 0.04	0.54 ± 0.010	0.77 ± 0.05	0.66 ± 0.011
	a_2 (%)	75.0 ± 2.82	0.73 ± 0.015	12.6 ± 2.09	0.92 ± 0.002
	k_2 (h^{-1})	$3.7 \times 10^{-4} \pm 6.7 \times 10^{-5}$	0.50 ± 0.016	$2.1 \times 10^{-2} \pm 2.1 \times 10^{-4}$	0.75 ± 0.006
	a_3 (%)			69.4 ± 3.60	0.94 ± 0.001
	k_3 (h^{-1})			$2.3 \times 10^{-4} \pm 3.3 \times 10^{-5}$	0.81 ± 0.004
	Model r^2	0.979 ± 0.002		0.999 ± 0.0001	
	I/M (%)	76.8 ± 2.39		82.0 ± 1.48	
Glucose	a_1 (%)	13.7 ± 0.67	0.52 ± 0.010	10.7 ± 0.61	0.69 ± 0.015
	k_1 (h^{-1})	0.24 ± 0.02	0.54 ± 0.002	0.73 ± 0.14	0.67 ± 0.009
	a_2 (%)	84.6 ± 0.74	0.77 ± 0.011	7.78 ± 0.46	0.92 ± 0.006
	k_2 (h^{-1})	$1.7 \times 10^{-4} \pm 3.3 \times 10^{-5}$	0.57 ± 0.018	$2.2 \times 10^{-2} \pm 4.6 \times 10^{-4}$	0.76 ± 0.012
	a_3 (%)			81.5 ± 0.91	0.94 ± 0.011
	k_3 (h^{-1})			$1.6 \times 10^{-4} \pm 4.0 \times 10^{-5}$	0.83 ± 0.025
	Model r^2	0.981 ± 0.001		0.999 ± 0.0001	
	I/M (%)	86.0 ± 0.68		89.3 ± 0.60	

observed for the double decay model ($P < 0.001$; see supplementary on-line material for further information, and Figs. S2, S3, S4 & S5 for double and triple exponential decay model fits with increasing number of data points, for alanine and glucose respectively).

For alanine, ^{14}C allocation to the first mineralizable pool showed no difference between the double and triple exponential models (i.e. pools a_1 and a_4; $P > 0.05$; Tables 2 and S1 for triple and double models respectively). However, the double exponential decay model produced half-lives twice as long as those for the triple decay model for this first pool ($P < 0.01$; Tables 2 and S1 for double and triple models respectively), with values of 0.10 ± 0.01 d and 0.04 ± 0.002 d for the triple and double models respectively. For ^{14}C-glucose, attribution of ^{14}C to pools a_1 and a_4 was similar and differed by only 3% with the double exponential decay model having higher values ($P < 0.05$; Tables 3 and S1 for triple and double models respectively). Half-lives for these pools were three times longer for the double exponential decay model (0.12 ± 0.01 d) in comparison to the triple exponential model (0.04 ± 0.01 d; $P < 0.01$; Tables 3 and S1 for triple and double models respectively).

Pool sizes for the second mineralizable pool (a_2 and a_5 for the triple and double model respectively) differed for both alanine and glucose ($P < 0.001$; Tables 2 and 3 and S1) between the two models. Values from the triple exponential decay model for alanine were approximately 60% lower than those for the double exponential decay model. Glucose showed greater disparity between the two models with the three pool model showing approximately 75% less apportionment to this pool in comparison to the two pool model. Rate constants for this pool (k_2 and k_5 for the three and two pool model respectively) were two-orders of magnitude shorter for the three pool model than the two pool model for both alanine and glucose ($P < 0.01$).

We also compared model parameters from the third mineralizable pool (a_3 and k_3) taken from the triple exponential model, with parameters from the second pool from the double model (a_5 and k_2). Results showed no significant difference ($P > 0.05$) between any model parameters or pool half-life.

Using the Newton–Raphson algorithm, total substrate halving-time was determined for each ^{14}C-substrate for both models. Overall, there were no differences in total substrate halving-time between the different models ($P > 0.05$). Alanine-derived C had a total substrate halving-time of 52.7 ± 9.6 d and 62.7 ± 16.0 d for the two and three pool models respectively. Total substrate halving-time for glucose-derived C was calculated as 151.3 ± 33.8 d and 154.4 ± 54.1 d for the two and three pool models respectively.

After combustion of the soil at the end experiment, we calculated that 64.8 ± 2.2% of the alanine ^{14}C remained unmineralized compared to 64.5 ± 9.6% for glucose. This was not significantly different to what we estimated to be remaining after accounting for the amount captured as $^{14}CO_2$ from the exponential decay models (51.9 ± 4.8% and 69.5 ± 3.1% activity remaining in soil, for alanine and glucose respectively; $P > 0.05$).

Table 5
Parameter estimates for the new integrated C pool model describing the flow of substrate-derived C through the soil microbial biomass and its subsequent mineralization. Values represent means ± 95% confidence intervals derived from the new model ($n = 3$). n/a indicates not applicable.

	Model parameters	Mean estimate from new model	Half-lives (d)
Alanine	k_{upt} (d^{-1})	246.5 ± 110.4	0.003
	$k_{ins,f}$ (d^{-1})	133.3 ± 6.4	0.005
	$k_{ins,b}$ (d^{-1})	57.2 ± 3.2	0.012
	k_{res_c} (−)	0.23 ± 0.03	3.08
	k_a (d^{-1})	322.4 ± 182.9	0.002
	k_d (d^{-1})	5027 ± 2961	1.4×10^{-4}
	b (d)	0.01 ± 0.01	n/a
Glucose	k_{upt} (d^{-1})	256.2 ± 19.7	0.003
	$k_{ins,f}$ (d^{-1})	104.7 ± 4.2	0.007
	$k_{ins,b}$ (d^{-1})	51.9 ± 2.1	0.013
	k_{res_c} (−)	0.11 ± 0.03	6.42
	k_a (d^{-1})	n/a	n/a
	k_d (d^{-1})	n/a	n/a
	b (d)	0.01 ± 0.01	n/a

3.7. Relationship between the size and turnover of soil solution, microbial biomass and $^{14}CO_2$ pools

Model parameters describing the depletion of substrate from soil solution, showed no agreement with rate constants describing the turnover of the first mineralization pool (a_1) from the triple exponential decay model for both substrates ($P < 0.001$). Half-lives for the soil solution pool were much shorter (0.003 ± 0.0002 d) for both substrates, than for the first pool (a_1) from the triple decay model (0.04 ± 0.01 d; $P < 0.01$).

We also compared model parameters obtained from combining results from soluble microbial biomass extractions (not corrected for k_{ec}) and the MeOH extractable pool, and applied a double exponential model to the data. These two pools were combined because they both represent extractable fractions of the microbial biomass. Model outputs were compared to those obtained from the triple exponential decay model describing $^{14}CO_2$ evolution.

The rate constants describing the turnover of the first mineralization pool for alanine only, showed no difference when compared to the first pool of the combined biomass pools ($P > 0.05$), but this

most likely reflects the high variability seen within the rate constants associated with the combined biomass pools for this substrate. Rate constants from the second and third mineralizable pools of the triple exponential decay model were significantly different to parameters from the first phase from the combined biomass pools, suggesting no relationship between these parameters ($P < 0.05$).

Glucose showed the opposite trend to alanine, with the rate constant associated with the first mineralizable pool from the triple exponential decay model being strongly different ($P < 0.001$) compared to the combined biomass rate constant from the first pool. However, the second and third pools from the triple exponential decay model, showed no differences when comparing rate constants from the combined biomass model ($P > 0.05$).

3.8. Results from the new integrated C flow model

Fig. 4 shows that the new integrated C flow model fitted well to our experimental data ($r^2 = 0.98$ for alanine and 0.97 for glucose). We see that sorption of the substrate to the soils solid phase only plays a minor part and does not limit respiration. Glucose does not sorb at all, and the buffer power for alanine ($k_a/k_d = 0.06$) is very small. Most of the ^{14}C-labelled substrate is rapidly taken up by the microbial biomass with an uptake rate constant that is an order of magnitude larger than the initial respiration rate constant (with $k_{upt} = 246$ d^{-1} and 256 d^{-1} for alanine and glucose respectively, compared to $k_{res\_t} = 15.8$ d^{-1} and 9 d^{-1} for alanine and glucose respectively; Table 5). Correspondingly, a large fraction of the ^{14}C is immobilised in the microbial biomass for the full duration of the experiment. For both glucose and alanine, the soluble and insoluble biomass pools tend towards an equilibrium, where approximately twice as much ^{14}C-labelled substrate was partitioned to insoluble biomass as determined by the ratios between $k_{ins,f}$ and $k_{ins,b}$. A full list of respiration rate constants (k_{res_t}) from the new model are presented in supplementary online material (Table S2). Our new model shows two distinct phases in CO_2 efflux, with a rapid initial respiration phase between 0 and 1 d after addition of the labelled substrates. After 1 d, the rate coefficients (k_{res_t}) remain fairly constant.

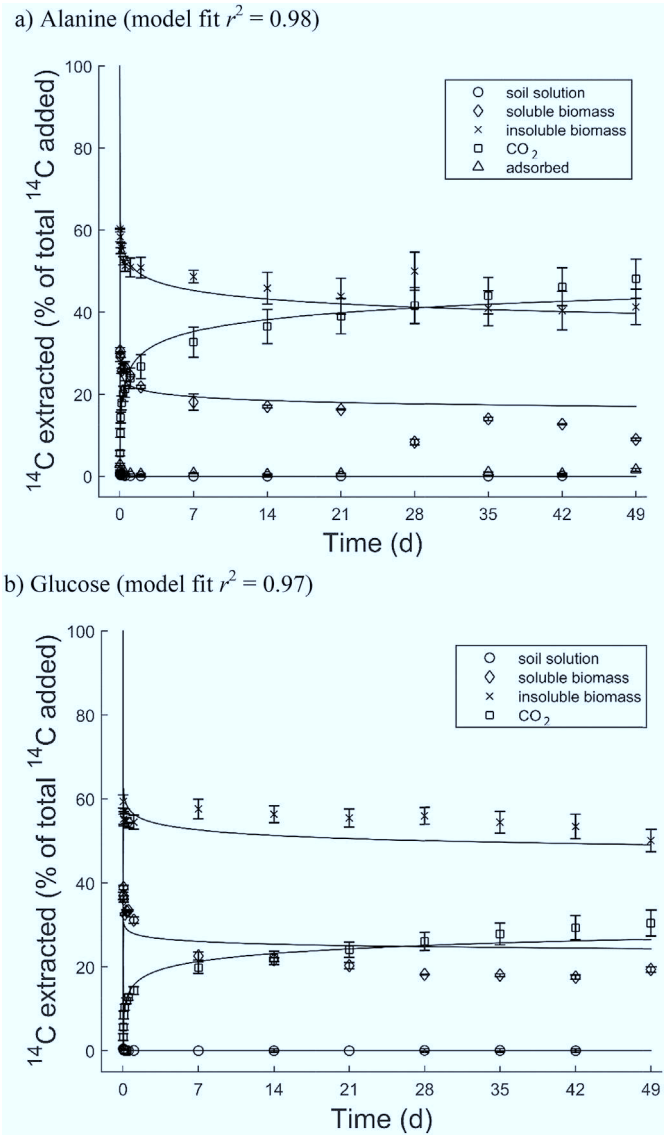

Fig. 4. New integrated C model describing the flow of substrate-derived C through the soil microbial biomass and its subsequent mineralization. The graphs show the amount of ^{14}C recovered from our experimental measures of different chemical extractions and cumulative microbial respiration (symbols) and our newly developed C model best fit lines for each extraction (solid lines). Values represent each individual replicate for the experimental data (open circles), whereas the model fit lines represents mean values ($n = 3$). Panel a shows experimental and modelled data for alanine and panel b is for glucose. The different symbols represent each chemical extraction. For all extractions used to parameterise the model, $n = 3$.

4. Discussion

4.1. Microbial uptake and sorption of the added substrates

The loss of both substrates from soil solution was extremely rapid with half-lives < 0.5 h. This suggests a very high C flux through the soil solution, particularly in comparison to the subsequent flux of substrate-derived C through the biomass. In agreement with Hill et al. (2008, 2012), a very simple model successfully described the microbial uptake of substrate from soil solution. Of the ^{14}C-substrate added to the soil, sorption to the solid phase only accounted maximally for <4% of the total (<1% after 1 h), indicating that this process had minimal influence on the microbial uptake of glucose or alanine (Fischer et al., 2010).

4.2. Estimating microbial C assimilation

Almost all of the added ^{14}C was rapidly taken up by the microbial community (>99% after 1 h). $CHCl_3$ fumigation-extraction and an additional methanol extraction, however, failed to recover all of the ^{14}C present in the biomass. The incomplete recovery of ^{14}C from the biomass supports the need to apply a k_{ec} correction factor if a full isotopic mass balance is required. The method we used to calculate k_{ec} makes the assumption that all of the ^{14}C not accounted for in soluble soil pools or respiratory losses, was located in the microbial biomass. In our opinion, this assumption is likely to be valid for the early part of the experiment. After longer incubation times, incorporation of a small amount of ^{14}C into non-microbial SOM pools may lead to a slight underestimation of k_{ec} (Jenkinson et al., 2004). Nevertheless, it is clear even from the first 24 h of incubation that the k_{ec} value was both critically dependent upon substrate incubation time and appeared substrate specific. This is accordance with estimates made following much higher substrate addition rates (Bremer and van Kessel, 1990). We therefore conclude that the use of k_{ec} correction factors in isotopic tracer studies is frequently invalid and their future use should be interpreted with considerable caution. In our opinion, the argument will also hold true for the equivalent use of k_{ec} values in other isotopic (e.g. ^{13}C and ^{15}N) tracer studies.

4.3. Critical evaluation of the modelling approach

Our aim was to identify a kinetic model which accurately describes the dynamics of CO_2 evolution arising from microbial uptake, assimilation and mineralization of C substrates. Mineralization of simple C compounds is frequently assumed to follow a biphasic pattern (Saggar et al., 1996; Chotte et al., 1998; Van Hees et al., 2005). Our results confirmed that a two pool model passed the specified statistical criteria and gave a reasonable fit to the experimental data, at least in the short term (<48 h). However, after 48 h and certainly at 49 d, this model was clearly too simple and a three pool model proved far superior, supporting the previous findings of Nguyen and Guckert (2001) and Farrar et al. (2012).

A good mathematical fit, however, does not imply that the model has any biological relevance and ascribing biological functionality to different pools is fraught with potential error. It is therefore critical that the results are not over interpreted. The triple exponential decay model for substrate mineralization, infers there are three distinct mineralizable pools into which substrate C is partitioned once it is added to the soil and subsequently taken up into the cell. Fundamentally, the model assumes (i) that these pools are progressively depleted independently of each other, and (ii) that the isotopic dilution is the same for all pools (Fig. 5a). In soil, however, these assumptions are almost certainly not valid for the following reasons (with specific reference to the three pool model):

a) The model assumes that C partitioning and assimilation rate is similar throughout the community. Although the kinetics of the transporters driving substrate uptake from soil may be similar within a diverse microbial community (Dijkstra et al., 2011), the expression of individual metabolic pathways within the cell undoubtedly varies depending on both differences in underlying physiology (e.g. eukaryote vs. prokaryote) and local microsite conditions. Given such complexity, it is surprising that simple models describe data as well as they do. However, complexity represents a problem when assigning function to discrete pools. In addition, microbial process rates will vary across the community. This is supported by studies showing temporal variation in ^{13}C-substrate assimilation into PLFAs by different microbial groups (Dungait et al., 2011; Tavi et al., 2013). The implications of this are that the turnover times of individual organisms for the process represented by pool a_1 (energy production), for example, may start to overlap with those of pool a_2 (short-term C storage) (Fig. 5b). This will lead to poor parameter estimates for the size and turnover rate of pools a_1 and a_2.

b) The model assumes that each pool describes a known suite of distinct biological processes. We fully accept that pools a_1, a_2, and a_3 comprise a multitude of different processes operating simultaneously within the community. Pool a_1 appears functionally quite distinct (rapid use of substrate for energy production). However, large uncertainty exists in the separation of pools a_2 and a_3 (as evidenced from the statistical criteria). It is clear that more pools and processes could be included. However, the resulting outputs would be largely meaningless on statistical grounds (data not presented). There is therefore a high degree of uncertainty associated with the parameter estimates for pools a_2 and a_3 and their associated rate constants and they should be interpreted with caution. The interpretation of the results would also benefit from ascribing a function to these pools. Combined for both substrates, the $CHCl_3$-fumigation-extraction (CFE) results, respiratory pool a_2 has a half-life similar to the first soluble CFE pool ($t_{½}$ 1.4 vs. 1.0 d), whilst respiratory pool a_3 has a similar half-life to the second soluble CFE pool ($t_{½}$ 172 vs. 107 d) and the second MeOH extractable pool ($t_{½}$ = 135 d). Thus respiratory pool a_3 probably reflects the turnover of both soluble (e.g. core metabolic enzymes) and insoluble structural elements (e.g. lipids, peptidoglycan) within the microorganisms upon death. Respiratory pool a_2 may therefore reflect a short-lived energy storage pool. It should, however, be considered that the attribution of pools to biological function may change with the duration of incubations. For instance, in long incubations (e.g. >49 d) the pool turning over most slowly may become more representative of slow turnover of quasi-stable soil C than of microbial C. However, this could be substrate specific and influenced by soil physical, chemical and biological factors (Van Hees et al., 2005).

c) The model assumes that the different C pools are depleted independently of each other. Based on the discussion above it is likely that the isotopic label contained in pool a_2 must pass back through a_1 before it is mineralized (Fig. 5c). This therefore underestimates the importance of pool a_1 and possibly its turnover rate depending on the pool linkages.

d) The model assumes the same rate of isotopic dilution within the three pools. Unfortunately, we know little about the size of the pools the isotopic label enters. However, we hypothesize that pool a_1 is very small in size and receives a disproportionately high level of isotopic labelling, overemphasizing its importance relative to pools a_2 and a_3. This is supported by the low concentration of respiratory metabolites in the cell relative to the rate of flux. In contrast, pool a_3 represents the structural components of the cell and will likely receive low isotopic enrichment (Fig. 5d). Despite its slow turnover, it may actually represent a much larger C flux. This problem is exacerbated when the added isotopically-labelled substrate has a low concentration relative to the C content of the microbial community (as performed here). While higher pulse additions may give better uniform enrichment across the three pools (as the isotope is used for generating new cells where all components are labelled), this will likely induce microbial growth, cause changes in community structure and thus poorly reflect natural C cycling processes.

e) The model assumes that C turnover takes place within the same organism. It is probable that pools a_1 and a_2 are turned over in response to general cell maintenance, however, pool a_3 may be turned over by a combination of mechanisms including: (i) direct consumption and breakdown by grazers (e.g. protozoa), and (ii) cell death and breakdown via extracellular enzymes releasing soluble products which are re-assimilated by neighbouring organisms. In both scenarios, a large proportion of the C may again enter a second set of long-lived C pools (Fig. 5e). While the amount of C allocated to pool a_3 will be correct, the rate constant describing its turnover will be vastly underestimated.

f) The model outputs are only as good as the experimental data. We clearly show that the duration and number of data points taken from the experiment strongly influenced the final model parameter estimates. In our view, the first mineralization phase of the two and three pool models (i.e. a_1 and a_4) represents the same flux and therefore their parameter estimates should be identical. It is reassuring that these rate constants do agree when interpreted appropriately (i.e. two pool model for experiments <48 h in length and three pool model for experiments >48 h: Figs. S2, S3, S4 & S5).

4.4. New model interpretation and comparison with triple exponential decay model

Models looking at C mineralization dynamics by the microbial biomass similar in style to our new model have been published (e.g. Nguyen and Guckert, 2001). However, they generally fail to include a feedback component between the different pools. They also alter the intrinsic soil solution pool by relatively high rates of substrate addition, which may stimulate microbial growth (Whitmore, 1996; Nguyen and Guckert, 2001; Blagodatsky et al., 2010). We have developed a new integrated model, using our empirical data to

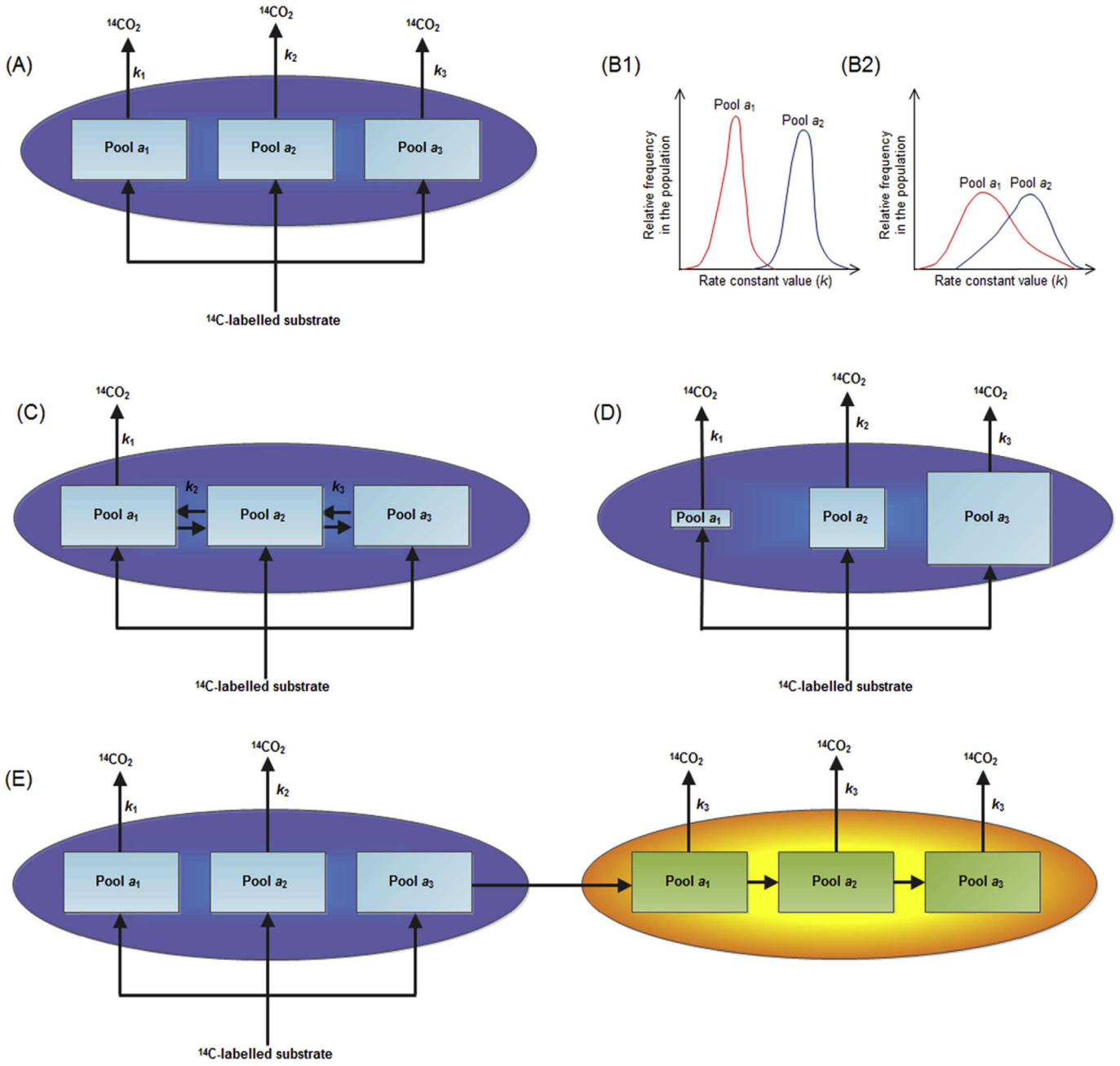

Fig. 5. Schematic representation of the different ways in which isotopically-labelled ^{14}C can flow through the microbial biomass. See Section 4.3 for more detail on the characteristics of the different models. Panel (A) shows the flow of isotopic C assuming that the C enters the microbial biomass and is partitioned into three discrete pools which are turned over independently. Panel (B) shows the distribution of rate constant values across the microbial community in a situation where all the community metabolises the C at similar rates leading to a clear separation of the kinetic pools a_1 and a_2 (Panel B1) or at different rates leading to poor resolution of the two kinetic pools (Panel B2). Panel (C) shows a representation of the model where the three pools (a_1, a_2 and a_3) are not independent but where the pools are interconnected with all C leaving via pool a_1. Panel (D) shows the situation where the intrinsic pools have different C contents leading to differences in isotope pool dilution. Panel (E) shows the situation where the originally labelled cell is predated by another microorganisms leading to C leaving pool a_3 and entering a new set of multiple pools in a different organism. These situations are not exhaustive and accurate description of isotope flow may be best described by a composite of different situations (e.g. Panels C, D and E).

address the issue of microbial processing of C within discrete pools with a level of connectivity between the different pools at conditions not inducing microbial growth.

This is something which cannot be achieved using simple exponential decay models (i.e. Eqns. (1) and (2)), therefore, we applied a set of new, independent equations to account for feedback between measured pools. Initially, we experimented with fitting a constant respiratory rate constant to our data within our new model, as used in a short 60 min incubation by Nguyen and Guckert (2001). However, this produced unacceptable fits to our data over our longer 49 d incubation, with the model failing to account for the slower dynamics observed after 2 days. Therefore, we had two values for the respiration rate constant; a larger one which represented well the early dynamics and a smaller one to best describe the later dynamics. Interestingly, Blagodatsky et al. (2010) also observed a similar phenomenon that the first three days of their 50 day investigation could not be well represented by the model and concluded that their simplistic model was not able

to capture the rapid glucose transport in microbial cells. Consequently, we investigated the idea that changes in the chemical nature of the introduced isotopic C tracer can result in a time-varying respiration rate constant (Bosatta and Ågren, 1995; Manzoni et al., 2012). Introducing a time-dependent respiration constant strongly improved the fit. Although we are aware that variation in the rate constant may actually reflect the dynamics of unmeasured pools upstream of respiration *per se*, using this approach, we could accurately reproduce the rapid initial phase of C accumulation in the biomass and respiration that we observed with our experimental data. The amount of substrate-C contained within the biomass is constrained by uptake (input) versus respiration rate (output). The model replicated the gradual accumulation of ^{14}C-labelled substrate in the microbial biomass due to the uptake rate constant being approximately twice as high as the initial respiration rate constant. Outputs from the model, suggest that the rate constants obtained from the triple exponential model, underestimate the respiration flux, as implied by the higher *k*-values from this model. This is not surprising given the simplicity of exponential decay models which attempt to describe a complex set of simultaneously occurring processes (as described above). Despite the lack of absolute agreement, the results are not that dissimilar from the triple exponential model, being within the same order of magnitude. For example, for alanine the first value of k_{res_t} is 0.66 h^{-1}, which is in the same order of magnitude as the rate constant of the first pool (k_1) from the triple exponential decay model 0.77 h^{-1}. The end value of k_{res_t} and the rate constant of the third pool (k_3) from the triple exponential model are also in the same order, with both at 0.0002 h^{-1}. The rate constant of the second pool (k_2) of the triple exponential decay model can also be found within the range of k_{res_t} from the new model, after approximately 0.5 d. Values for glucose are also similar. The first k_{res_t} value is 0.38 h^{-1}, compared with 0.73 h^{-1} for the first pool (k_1) from the triple exponential decay model. The final k_{res_t} value again matches well with 0.0001 h^{-1}, compared to 0.0002 h^{-1} for the third pool (k_3) from the triple exponential decay model. The rate constant for the second pool (k_2) of the triple exponential decay model can also be found within the k_{res_t} ranges from the new model, after approximately 0.25 d. This implies that outputs from a triple exponential model may still be useful in estimating respiration, but that interpretation of the biological meaning of the different pools needs to be made with caution. Our new model is more realistic in terms of specific microbial pools and their interactions. It also explicitly considers the microbial biomass whereas the triple exponential model does not.

4.5. Recommendations for model interpretation

Despite the caveats identified above, we can make clear recommendations on the use and interpretation of the modelling approaches for evaluating the turnover of simple C substrates in soil:

1. At realistic substrate concentrations, the turnover of the fast respiratory pool of exponential decay models (a_1) does not approximate depletion from the soil solution. The use of k_1 to estimate substrate depletion would underestimate substrate turnover rates in soil solution by 20-fold. If the flux of C compounds through soil solution is required, then an alternative approach is required (e.g. depletion approach described here and in Hill et al., 2008).

2. The choice of model should clearly match the duration of the experiment to avoid either under- or over-fitting of the data. Essentially, the longer the incubation time the more complex the model required. For example, if applying an exponential decay model, short-term incubations (<48 h) should use a two pool model while longer-term incubations should use a three pool model.

3. There is a high degree of confidence in the assessment of the size and rate of turnover for pool a_1 of exponential decay models which allows direct comparison of different experimental treatments. In contrast, problems in isotopic pool dilution and pool connectivity make the values obtained for pool a_3 extremely uncertain. If used at all, these values will only ever provide crude estimates of C turnover within the biomass.

4. Our new integrated model provides a more realistic estimate of microbial substrate turnover encompassing some of the more complex interactions between different C pools, rather than using simpler exponential decay models. In addition, it may also be changed/extended if required, i.e. if there are other data or new information to include.

5. Chloroform-fumigation extraction represents a poor technique for assessing the amount of isotope contained in the microbial biomass. The incomplete extraction of the biomass and the continually changing k_{ec} values makes the data essentially uninterpretable.

5. Conclusions

Isotope pulse labelling is widely employed both in the laboratory and field to investigate the flow of C and N through soil ecosystems. In this study, we critically evaluated the combined use of experimental ^{14}C labelling and mathematical modelling to estimate C turnover times in soil. We conclude that the technique is frequently used inappropriately, particularly when using the chloroform fumigation-extraction technique to quantify the amount of ^{13}C/^{14}C immobilised by the microbial biomass. Further, the traditional mineralization approach provides poor estimates of substrate loss from soil solution with the model outputs mostly reflecting rates of internal C metabolism within the microbial cells. Choice of the exponential decay model which best describes substrate-C turnover in soil is influenced by a range of factors including (1) substrate type, (2) the duration of the experiment, (3) whether the allocated C pools have any biological meaning, and (4) whether the model can be validated. Therefore, while isotope addition provides a simple mechanism for labelling the microbial biomass, it provides limited information on the behaviour of the substrate itself. For longer term isotope labelling studies (>48 h) a three pool model is most appropriate to describe C mineralization and here we ascribe gross functions to these three pools which will aid in future interpretation. However, due to problems of pool connectivity and isotopic pool dilution it is difficult to use the model quantitatively to describe C loss rates from soil.

Our new empirical data provides a much better and more realistic estimate of microbial substrate use and in turn respiration flux from the microbial biomass. Respiration rate constants from the new model were remarkably similar to outputs from the triple exponential model implying that exponential models may still useful in estimating respiration, but that interpretation of the biological meaning of the different pools needs to be made with caution. Recent advances in metabolomic technology are likely to offer new opportunities for understanding the fate of individual substrates in soil particularly when used in combination with other techniques such as transcriptomics and stable isotope proteomics.

Acknowledgments

This work was funded by the UK Natural Environment Research Council. We thank Francis Guyver and Matthew Harris for helping with laboratory analysis. We thank Mark Farrell for his assistance with the planning of this study. We also thank Richard Quilliam and

Harriet Orr for their assistance with the manuscript and figures. Andrea Schnepf thanks the Austrian Science Fund FWF (Grant No.: V220-N13).

Appendix A. Supplementary data

Supplementary data related to this article can be found at http://dx.doi.org/10.1016/j.soilbio.2015.11.016.

References

Aldén, L., Demoling, F., Bååth, E., 2001. Rapid method of determining factors limiting bacterial growth in soil. Applied and Environmental Microbiology 6, 1830–1838.

Allison, S.D., Martiny, J.B.H., 2008. Resistance, resilience, and redundancy in microbial communities. Proceedings of the National Academy of Sciences (PNAS) 105, 11512–11519.

Barber, S.A., 1984. Soil Nutrient Bioavailability. A Mechanistic Approach. Wiley and Sons, Inc., London.

Berner, R.A., 1964. An idealised model of dissolved sulphate distribution in recent sediments. Geochemica et Cosmochimica Acta 28, 1497–1503.

Blagodatsky, S., Blagodatskaya, E., Yuyukina, T., Kuzyakov, Y., 2010. Model of apparent and real priming effects: linking microbial activity with soil organic matter decomposition. Soil Biology & Biochemistry 42, 1275–1283.

Boddy, E., Hill, P.W., Farrar, J., Jones, D.L., 2007. Fast turnover of low molecular weight components of the dissolved organic carbon pool of temperate grassland field. Soil Biology & Biochemistry 39, 827–835.

Bosatta, E., Ågren, G., 1995. The power and reactive continuum models as particular cases of the *q*-theory of organic matter dynamics. Geochimica et Cosmochimica Acta 59, 3833–3835.

Bremer, E., van Kessel, C., 1990. Extractability of microbial ^{14}C and ^{15}N following addition of variable rates of labelled glucose and $(NH_4)_2SO_4$ to soil. Soil Biology & Biochemistry 22, 707–713.

Chotte, J.L., Ladd, J.N., Amato, M., 1998. Sites of microbial assimilation, and turnover of soluble and particulate ^{14}C-labelled substrates decomposing in a clay soil. Soil Biology & Biochemistry 30, 205–218.

Coody, P.N., Sommers, L.E., Nelson, D.W., 1986. Kinetics of glucose uptake by soil microorganisms. Soil Biology & Biochemistry 18, 283–289.

Crawley, M.J., 2007. The R Book. John Wiley and Sons Ltd., Chichester, England.

Dictor, M.C., Tessier, L., Soulas, G., 1998. Reassessment of the K_{EC} coefficient of the fumigation-extraction method in a soil profile. Soil Biology & Biochemistry 30, 119–127.

Dijkstra, P., Thomas, S.C., Heinrich, P.L., Koch, G.W., Schwartz, E., Hungate, B.A., 2011. Effect of temperature on metabolic activity of intact microbial communities: evidence of altered metabolic pathway activity but not for increased maintenance respiration and reduced carbon use efficiency. Soil Biology & Biochemistry 43, 2023–2031.

Dungait, J.A.J., Kemmitt, S.J., Michallon, L., Guo, S., Wen, Q., Brookes, P.C., Evershed, R.P., 2011. Variable responses of the soil microbial biomass to trace concentrations of ^{13}C-labelled glucose, using ^{13}C-PLFA analysis. European Journal of Soil Science 62, 117–126.

Farrar, J., Boddy, E., Hill, P.W., Jones, D.L., 2012. Discrete functional pools of soil organic matter in a UK grassland soil are differentially affected by temperature and priming. Soil Biology & Biochemistry 49, 52–60.

Fischer, H., Ingwersen, J., Kuzyakov, Y., 2010. Microbial uptake of low-molecular-weight organic substances out-competes sorption in soil. European Journal of Soil Science 61, 504–513.

Fujii, K., Hayakawa, C., van Hees, P.A.W., Funakawa, S., Kosaki, T., 2010. Biodegradation of low molecular weight organic compounds and their contribution to heterotrophic soil respiration in three Japanese forest spoils. Plant Soil 334, 475–489.

Giesler, R., Lundström, U., 1993. Soil solution chemistry: effects of bulking soil samples. Soil Science Society of America Journal 57, 1283–1288.

Gill, R.A., Jackson, R.B., 2000. Global patterns of root turnover for terrestrial ecosystems. New Phytologist 147, 13–31.

Glanville, H., Rousk, J., Golyshin, P., Jones, D.L., 2012. Mineralization of low molecular weight carbon substrates in soil solution under laboratory conditions. Soil Biology & Biochemistry 48, 88–95.

Hanson, P.J., Edwards, N.T., Garten, C.T., Andrews, J.A., 2000. Separating root and soil microbial contributions to soil respiration: a review or methods and observations. Biogeochemistry 48, 115–146.

Harakuk, O., Smith, M.J., Luo, Y., 2015. Microbial models with data-driven parameters predict stronger soil carbon responses to climate change. Global Change Biology 21, 2439–2453.

Hill, P.W., Farrar, J.F., Jones, D.L., 2008. Decoupling of microbial glucose uptake and mineralization in soil. Soil Biology & Biochemistry 40, 616–624.

Hill, P.W., Farrell, M., Roberts, P., Farrar, J., Grant, H., Newsham, K.K., Hopkins, D.W., Bardgett, R.D., Jones, D.L., 2011. Soil- and enantiomer-specific metabolism of amino acids and their peptides by Antarctic soil microorganisms. Soil Biology & Biochemistry 43, 2410–2416.

Hill, P.W., Farrell, M., Jones, D.L., 2012. Bigger may be better in soil N cycling: does rapid acquisition of small L-peptides by soil microbes dominate fluxes of protein-derived N in soil? Soil Biology & Biochemistry 48, 106–112.

Jenkinson, D.S., Brookes, P.C., Powlson, D.S., 2004. Measuring soil microbial biomass. Soil Biology & Biochemistry 36, 5–7.

Joergensen, R.G., Wu, J., Brookes, P.C., 2011. Measuring soil microbial biomass using an automated procedure. Soil Biology & Biochemistry 43, 873–876.

Jones, D.L., Owen, A.G., Farrar, J.F., 2002. Simple method to enable the high resolution determination of total free amino acids in soil solutions and soil extracts. Soil Biology & Biochemistry 34, 1893–1902.

Jones, D.L., Dennis, P.G., Owen, A.G., van Hees, P.A.W., 2003. Organic acid behaviour in soils – misconceptions and knowledge gaps. Plant and Soil 248, 31–41.

Jones, D.L., Willet, V.B., 2006. Experimental evaluation of methods to quantify dissolved organic nitrogen (DON) and dissolved organic carbon (DOC) in soil. Soil Biology & Biochemistry 38, 991–999.

Jones, D.L., Nguyen, C., Finlay, R.D., 2009. Carbon flow in the rhizosphere: carbon trading at the soil-root interface. Plant and Soil 321, 5–33.

Kuzyakov, Y., 2006. Sources of CO_2 efflux from soil and review of partitioning methods. Soil Biology & Biochemistry 38, 425–448.

Manzoni, S., Piñeiro, G., Jackson, R.B., Jobbágy, E.G., Kim, J.H., Porporato, A., 2012. Analytical models of soil and litter decomposition: solutions for mass loss and time-dependent rates. Soil Biology & Biochemistry 50, 66–76.

Middleburg, J.J., 1989. A simple rate model for organic matter decomposition in marine sediments. Geochimica et Cosmochimica Acta 53, 1577–1581.

Miranda, K.M., Espey, M.G., Wink, D.A., 2001. A rapid, simple spectrophotometric method for simultaneous detection of nitrate and nitrite. Biology and Chemistry 5, 62–71.

Mulvaney, R.L., 1996. Nitrogen – inorganic forms. In: Sparks, D.L. (Ed.), Methods of Soil Analysis. Part 3. Soil Society of America Inc., Madison, WI, pp. 1123–1184.

Murphy, J., Riley, J.P., 1962. A modified single solution method for the determination of phosphate in natural waters. Analytica Chimica Acta 27, 31–36.

Myklestad, S.M., Skånøy, E., Hestmann, S., 1997. A sensitive and rapid method for analysis of dissolved mono-and polysaccharides in seawater. Marine Chemistry 56, 279–286.

Nguyen, C., Guckert, A., 2001. Short-term utilisation of ^{14}C-[U] glucose by soil microorganisms in relation to carbon availability. Soil Biology & Biochemistry 33, 53–60.

Nguyen, C., 2009. Rhizodeposition of organic C by plants: mechanisms and controls. In: Lichtfouse, E., Navarrete, M., Debaeke, P., Souchere, V., Alberola, C. (Eds.), Sustainable Agriculture, pp. 97–123.

Ostle, N.J., Smith, P., Fisher, R., Woodward, F.I., Fosher, J.B., Smith, J.U., Galbraith, D., Levy, P., Meir, P., McNamara, N.P., Bardgett, R.D., 2009. Integrating plant-soil interactions into global carbon cycle models. Journal of Ecology 97, 851–863.

Paul, E.A., 2007. Soil Microbiology, Ecology, and Biochemistry, third ed. Elsevier Inc., New York.

Roose, T., Schnepf, A., 2008. Mathematical models of plant-soil interaction. Philosophical Transactions of the Royal Society 366, 4597–4611.

Saggar, S., Parshotam, A., Sparling, G.P., Feltham, C.W., Hart, P.B.S., 1996. ^{14}C-labelled ryegrass turnover and residence times in soils varying in clay content and mineralogy. Soil Biology & Biochemistry 28, 1677–1686.

Salter, R.M., Green, T.C., 1933. Factors affecting the accumulation and loss of nitrogen and organic carbon in cropped soils. Journal of the American Society of Agronomy 25, 622–630.

Simfukwe, P., Hill, P.W., Emmett, B.A., Jones, D.L., 2011. Soil classification provides a poor indicator of carbon turnover rates in soil. Soil Biology & Biochemistry 43, 1688–1696.

Tavi, N.M., Martikainen, P.J., Lokko, K., Kontro, M., Wild, B., Richter, A., Biasi, C., 2013. Linking microbial community structure and allocation of plant-derived carbon in an organic agricultural soil using (CO_2)-^{13}C pulse-chase labelling combined with ^{13}C-PLFA profiling. Soil Biology & Biochemistry 58, 207–215.

Vance, E.D., Brookes, P.C., Jenkinson, D.S., 1987. An extraction method for measuring soil microbial biomass C. Soil Biology & Biochemistry 19, 109–707.

Van Hees, P.A.W., Jones, D.L., Finlay, R., Godbold, D., Lundström, U.S., 2005. The carbon we do not see – the impact of low molecular weight compounds on carbon dynamics and respiration in forest soils: a review. Soil Biology & Biochemistry 37, 1–13.

Van Hees, P.A.W., Johansson, E., Jones, D.L., 2008. Dynamics of simple carbon compounds in two forest soils as revealed by soil solution concentrations and biodegradation techniques. Plant and Soil 310, 11–23.

Velioglu, Y.S., Mazza, G., Gao, L., Oomah, B.D., 1998. Antioxidant activity and total phenolics in selected fruits, vegetables and grain products. Journal of Agricultural and Food Chemistry 46, 4113e4117.

Wallander, H., 2006. External mycorrhizal mycelia – the importance of quantification in natural ecosystems. New Phytologist 171, 240–242.

Whitmore, A., 1996. Describing the mineralization of carbon added to soil in crop residues using second-order kinetics. Soil Biology & Biochemistry 28, 1435–1442.

Wolfe, R.R., Chinkes, D.L., 2005. Isotope Tracers in Metabolic Research, second ed. John Wiley & Sons, Inc., London.

Wu, J., Joergensen, R.G., Pommerening, B., Chaussod, R., Brookes, P.C., 1990. Measurement of soil microbial biomass C by fumigation-extraction-an automated procedure. Soil Biology & Biochemistry 22, 1167–1169.